



OATAO is an open access repository that collects the work of Toulouse researchers and makes it freely available over the web where possible.

This is an author-deposited version published in : <http://oatao.univ-toulouse.fr/>  
Eprints ID : 9217

To link to this article : DOI: 10.1016/j.cej.2006.08.002  
URL : <http://dx.doi.org/10.1016/j.cej.2006.08.002>  
Open Archive TOULOUSE Archive Ouverte (OATAO)

To cite this version : Anne-Archard, Dominique and Marouche, Mohamed and Boisson, Henri-Claude *Hydrodynamics and Metzner-Otto correlation in stirred vessels for yield stress fluids.* (2006) Chemical Engineering Journal, vol. 125 . pp. 15-24. ISSN 1385-8947

# Hydrodynamics and Metzner–Otto correlation in stirred vessels for yield stress fluids

D. Anne-Archard\*, M. Marouche, H.C. Boisson

*Institut de Mécanique des Fluides de Toulouse, UMR CNRS-INP-UPS 5502, Allée du Professeur Camille Soula, 31400 Toulouse, France*

---

## Abstract

This paper investigates the hydrodynamics and power consumption in laminar stirred vessel flow using numerical computation. The Metzner–Otto correlation was established for mixing in power-law fluids. This paper focuses on its application to yield stress fluids. Distributions of shear rates and their link to power consumption for helical and anchor agitators are discussed. Insight is sought from the analytical formula for Taylor–Couette flows. Laws are established for Bingham, Herschel–Bulkley and Casson fluids and reveal similar results. Fully or partially sheared flow situations with plug regions are considered. Depending on the fluid model, the concept is valid or constitutes a satisfactory approximation for fully sheared flows. When the flow is partially sheared, the expression depends on the Bingham number and the concept must be adapted. The results of the numerical simulations are interpreted in the light of this analysis and results from the literature.

*Keywords:* Mixing; Energy; Fluid mechanics; Laminar flow; Non-Newtonian fluids; Numerical analysis

---

## 1. Introduction

Mixing operations with non-Newtonian fluids are frequently employed in areas such as the food, pharmaceutical, paint, or polymer industries. Additional difficulties for the optimization of processes often occur with such fluids. In fact, the hydrodynamics strongly depends on the nature of the fluids involved in the mixing system. Viscoplastic fluids (also called yield stress fluids) are an important class of non-Newtonian fluids. These fluids flow only when the shear stress is above a certain threshold, the yield stress, and this leads in particular to dead zones in the flow which lower mixing efficiency [1–3].

As a resulting global value of local hydrodynamics, power consumption is of particular interest, partly because it is easy to measure. Therefore it has always been a key parameter in all chemical engineering studies and it is examined in priority for every mixing system, whether in the industrial or the research environment. It is thus a fundamental parameter not only for determining the process operating cost but also for the process design. Non-Newtonian fluids and principally yield stress fluids are still poorly understood in this respect. In this case, experi-

mentation becomes more difficult partly because of unwanted wall slip and frozen regions in the vessel. For these specific reasons, numerical and analytical studies are the more appropriate means to obtain information about both the hydrodynamics and the nature of the power correlation.

The objective of this paper is two-fold: (i) to evaluate the power consumption for yield stress fluids in two standard mixing systems for highly viscous fluids and (ii) to test the possibility of applying an appropriate correlation between the power consumption and the non-dimensional flow parameters for chemical engineering purposes.

Such a correlation for Newtonian fluids in the laminar regime corresponds to a friction coefficient that is inversely proportional to the Reynolds number  $Re$ . For mixing systems, this property is written as

$$N_p Re = K_p, \quad (1)$$

where  $N_p$  is the power number proportional to power consumption  $P$ , and  $K_p$  is a geometric factor which characterizes the system. This relationship is frequently used in practice. It was then logical to extend it to non-Newtonian fluids. Metzner and Otto [4] did this in 1957 for shear thinning fluids (also referred to as pseudoplastic fluids) and their work has been an authority since then. In fact, the Reynolds number needs to be reconsidered

---

\* Corresponding author. Tel.: +33 561 285 890; fax: +33 561 285 992.  
E-mail address: Dominique.Anne-Archard@imft.fr (D. Anne-Archard).

## Nomenclature

$Bi$	Bingham number
$Bi^*$	transition Bingham number
$c$	agitator to wall clearance
$C$	torque
$C_1, C_2$	critical torque values (Taylor–Couette flow)
$\underline{D}$	rate of strain tensor
$\underline{D}, D_a$	impeller diameter
$H$	height of the fluid
$K$	Herschel–Bulkley model parameter
$K_c$	Casson model parameter
$K_p$	power constant
$K_s$	Metzner–Otto coefficient
$n$	power law index
$N$	rotation frequency
$N_p$	power number
$p$	pitch of the ribbon
$P$	power consumption
$r$	radial co-ordinate
$r^*$	non-dimensional radial co-ordinate
$R_1, R_2$	inner and outer radius (concentric cylinders)
$Re$	Reynolds number
$Re'$	critical Reynolds number
$Re_g$	generalized Reynolds number
$s$	radius ratio (Taylor–Couette geometry)
$T$	vessel diameter
$V_\theta, V_z$	tangential and axial velocity
$V^*$	non-dimensional velocity
$X_0$	non-dimensional radial co-ordinate for transition
$w$	impeller or ribbon width

### Greek letters

$\dot{\gamma}$	shear rate
$\dot{\gamma}_{\text{eff}}$	effective shear rate
$\eta_{\text{eff}}$	effective viscosity
$\eta_\infty$	Bingham model parameter (viscosity)
$\rho$	density
$\underline{\tau}$	stress tensor
$\tau_0$	yield stress
$\omega$	angular velocity

for non-Newtonian fluids, as the viscosity of the fluid is not constant but dependent on the shear rate. As Eq. (1) characterizes the laminar flow regime and must be retained in non-Newtonian laminar flows, it can be used to define a generalized Reynolds number. From this generalized Reynolds number, an effective viscosity  $\eta_{\text{eff}}$  can be deduced. Therefore,  $\eta_{\text{eff}}$  is defined as the viscosity of the Newtonian fluid providing the same power consumption as the non-Newtonian fluid for the studied system:

$$Re_g = \frac{\rho ND^2}{\eta_{\text{eff}}} \quad (2)$$

Metzner and Otto [4] introduced the concept of effective viscosity which is linked to an effective shear rate  $\dot{\gamma}_{\text{eff}}$  using the

rheological characterization of the fluid  $\eta(\dot{\gamma})$ . They suggested this effective shear rate to be proportional to the rotation frequency  $N$ :

$$\dot{\gamma}_{\text{eff}} = K_s N \quad (3)$$

They validated their hypothesis with helical screw and helical ribbon agitators. In 1996, Tanguy et al. [5] in their attempt to perform a numerical simulation of this problem presented a review of the literature relating to the major experimental works up to 1996. Numerous references also figure in the review by Doraiswamy et al. [6]. In fact, many authors deriving a correlation for power consumption in mixing systems have validated and adopted this concept for shear thinning fluids. Moreover, the variations of the Metzner–Otto parameter  $K_s$  with the power-law index  $n$  prove to be small for weakly shear thinning fluids and this justifies the approximation of a constant value. However Brito de la Fuente et al. [7], Carreau et al. [8] and Tanguy et al. [5] examining highly shear thinning fluids ( $n$  in the range 0.1–0.4) found a marked increase of  $K_s$  with  $n$  (helical ribbon impellers and anchor) in their experimental results, while Rieger and Novak [9] and Sestak et al. [10] observe strongly decreasing values. In fact, these results seem to demonstrate the fact that the value of  $K_s$  depends strongly on the rheology for highly shear thinning fluids.

Much less attention has been paid to mixing in viscoplastic fluids. The utility of the Metzner–Otto concept in such cases is debatable. The first published study seems to be by Nagata et al. [11] who were mainly interested in laminar-turbulence transition but also suggested a Reynolds-based condition for the existence of a shear-free region. Later, Hirata and Aoshima [2] focused their experimental approach on the variations of sheared regions ('caverns') with a generalized Reynolds number calculated using the Metzner–Otto concept. They justify this approach by the constant value of the fitted  $K_s$  parameter obtained in the laminar regime (with a Reynolds number in the range 1–10). Curran et al. [12] use the same approach for two viscoplastic fluids and two helical ribbon agitators. The fitted values of  $K_s$  are slightly different for the two fluids with the simple helical ribbon agitator, but they differ substantially with the double helical ribbon impeller. Hirata and Aoshima therefore suggest that  $K_s$  depends both on fluid rheology and on geometry. The mixing of viscoplastic fluids has also been studied using numerical simulations. Bertrand et al. [13] analyze an anchor impeller mixing system, Tanguy et al. [14] a twin-blade planetary mixer and Torrez and André [15] a Rushton turbine. These latter authors obtain  $K_s$  values which vary with fluid rheology from 7.3 to 9.6 while a generalized Reynolds number varies in the range 0.6–15. Conversely for the planetary mixer, Tanguy et al. [14] conclude that  $K_s$  variations can be put aside when the Bingham number is less than 40. However, for the anchor agitator mixing system, Bertrand et al. [13] present a detailed analysis for highly viscoplastic fluids and observe a weak increase of  $K_s$  from 21.1 to 23.8.

The present work studies two mixing systems specifically for viscoplastic fluids. Such a situation occurs for instance in an emulsion copolymerization process at high concentrations.

A rheological characterization of this emulsion has been performed by Marouche et al. [16]. The mixing systems investigated are flat-bottomed vessels equipped with double helical ribbon or anchor agitators as they are common systems for highly viscous fluids. The first part is devoted to CFD results. The numerical approach was previously validated on the Taylor–Couette flow for which analytical results are available (Marouche et al. [17]). The hydrodynamics of the mixing systems is presented here and we focus on the shear rate which is a key parameter for yield stress fluids. These results show the effect of viscoplasticity on the velocity field and on the shear rate field. They constitute the basis for the calculation of the power consumption which is studied in the second part of this paper. In this latter part, the relationship between the Metzner–Otto parameter (calculated from the power consumption) and the Bingham number is analyzed. It is first derived analytically for the Taylor–Couette flow. Sheared and non-sheared regions are characterized and their existence is related to power consumption. The power number is subsequently derived numerically for the mixing systems under study and the application of the Metzner–Otto concept to such standard systems is discussed.

## 2. Hydrodynamics and shear rate fields for yield stress fluids in mixing vessel

The two commonly used agitators for highly viscous fluids are helical ribbon and anchor. The latter, although not usual in industrial processes because of its low efficiency, is interesting because of the mainly tangential flow generated at low rotational speed, which makes the Taylor–Couette analogy possible (Ait-Kadi et al. [18]). Variations of the hydrodynamics and power consumption for such agitators have been extensively studied, for both Newtonian and non-Newtonian pseudoplastic fluids. To study the yield stress fluids which constitute the purpose of this paper, mixing systems are dealt with by numerical simulation using viscoplastic fluids modeled by a Bingham law:

$$\underline{D} = 0 \quad \text{for } |\underline{\tau}| \leq \tau_0 \quad (4)$$

$$\underline{\tau} = \left( \eta_\infty + \frac{\tau_0}{\dot{\gamma}} \right) \underline{D} \quad \text{for } |\underline{\tau}| \geq \tau_0 \quad (5)$$

where  $\underline{D}$  and  $\underline{\tau}$  are, respectively, the rate of strain tensor and the stress tensor.  $\tau_0$  is the yield stress and the shear rate  $\dot{\gamma}$  is defined as  $\dot{\gamma} = \sqrt{2 \text{tr } \underline{D}^2}$  where tr stands for the trace. A dimensionless number comparing yield stress to a viscous stress is defined through the Bingham number:

$$Bi = \frac{\tau_0}{\eta_\infty N} \quad (6)$$

Numerical simulation is conducted for both double helical ribbon and anchor agitator using the commercial CFD code FLUENT. A second order scheme is used for the pressure and for the momentum equations. The coupling velocity–pressure is processed by the SIMPLE algorithm. The computations are conducted in a rotating frame bound to the impeller so that the problem is steady. The Bingham model requires a numerical approximation to overcome infinite viscosity in shear-free regions. The

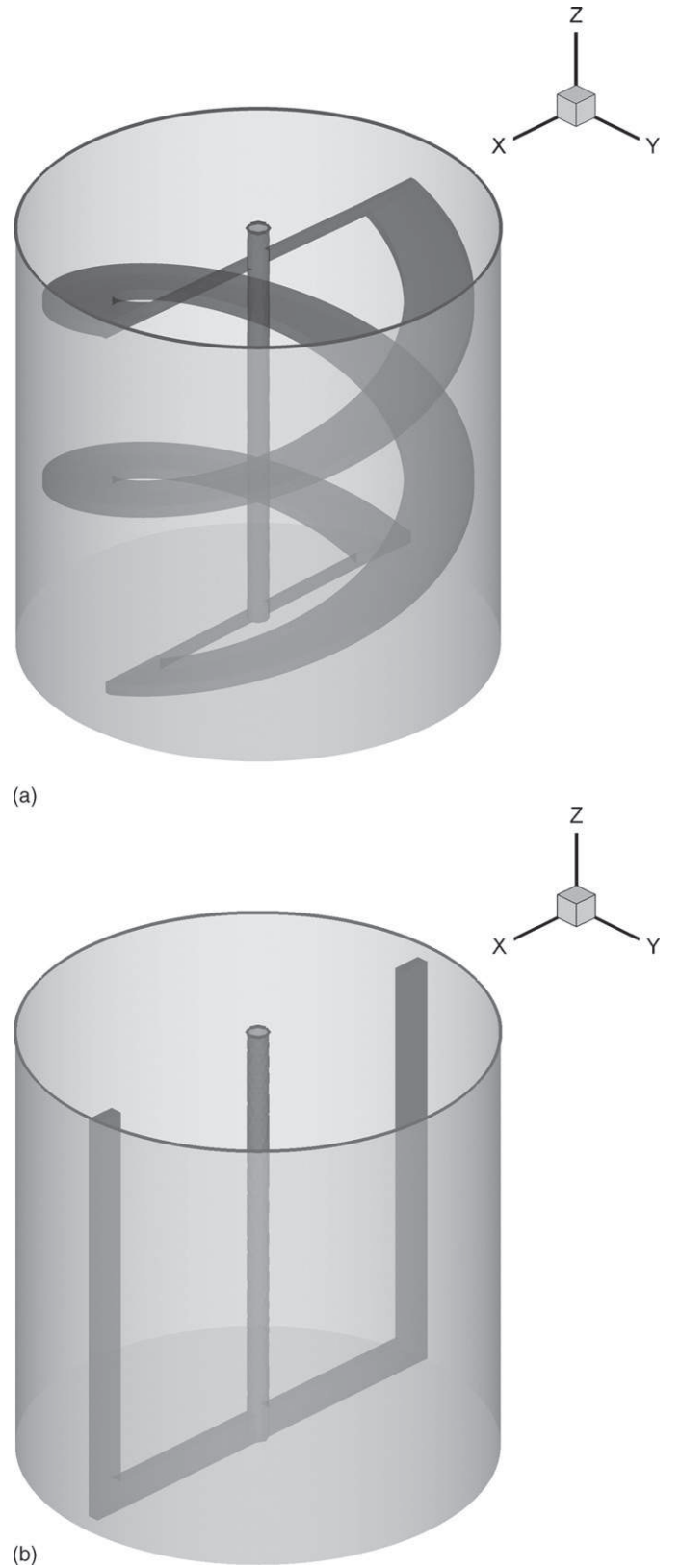


Fig. 1. Geometry of the mixing systems.

usual models for numerical approximation of Bingham fluid are the bi-viscosity model (Vradis and Otugen [19], O'Donovan and Tanner [20]), the Papanastasiou model (Papanastasiou [21], Pham and Mitsoulis [22]), the Bercovier and Engelman model [23] and the Carreau model with a very low power-law index (typically  $10^{-3}$ ) [17]. All these models have been implemented in the code by user-defined functions, apart from the Carreau model which is a standard option of FLUENT. These models were compared in the theoretical case of a Taylor–Couette flow. The difference with the analytical results was quantified on the velocity profile and especially on the critical region of sheared/unsheared transition. The parameters of the numerical procedure were chosen to set a final error level of less than 2% of the reference velocity. Both the comparison and the numerical procedure are described in Marouche et al. [17] and Marouche [24]. For the studied 2D and 3D mixing systems, the independence to both the mesh size and the approximation parameters is checked. It has been shown that these approximation parameters need to be adjusted when the Bingham numbers increase. Special attention is paid to this issue. The unstructured meshes used for the 3D anchor and helical ribbon systems consist of 692,825 and 700,218 tetrahedral cells, respectively.

The mixing systems are presented in Fig. 1a and b. The tank is a flat-bottomed vessel (inside diameter:  $T$ ) equipped with an anchor or a double helical ribbon agitator (diameter:  $D_a$ ). The anchor was treated in 2D and 3D and helical ribbon in 3D.  $H$  is the fluid height. Values for the impeller or ribbon width  $w$ , agitator-to-wall clearance  $c$  and pitch of the ribbon  $p$  are reported in Table 1. The double helical ribbon impeller is geometrically similar to the one used by Curran et al. [12] in their experimental study.

Numerical simulations were conducted for different Bingham numbers in the range 60–12,000 which were obtained using various yield stresses and various rotational speeds. As pointed out by Marouche et al. in the case of the 2D anchor agitator ([17,24]), the hydrodynamics can be strongly modified by yield stress. Similar effects are observed on the double helical ribbon: Figs. 2 and 3 present the non-dimensional radial profiles of the axial and tangential velocities taken at  $z = T/2$  and  $x = 0$  (using  $V^* = V/\pi NT$  and  $r^* = r/(T/2)$ ). As observed by Bertrand et al. [13], yield stress leads to markedly lower axial pumping (Fig. 2). Correlatively, tangential velocity seems to undergo acceleration when compared to the Newtonian reference case (Fig. 3). But it is noteworthy that the linearity of the profiles  $V_\theta^*(r^*)$  concerns a region that becomes larger as the Bingham number increases. This corresponds to lower velocity gradients in the radial direction. Yield stress then leads to higher velocities which are closer to the driven velocity of the agitator. This is confirmed by the graph in Fig. 4 which shows the reduced tan-

Table 1  
Geometrical characteristics for agitators

	$D_a/T$	$H/T$	$c/T$	$w/T$	$p/T$
Anchor	0.96	1	0.02	0.067	–
Double helical ribbon	0.89	1	0.055	0.144	0.89

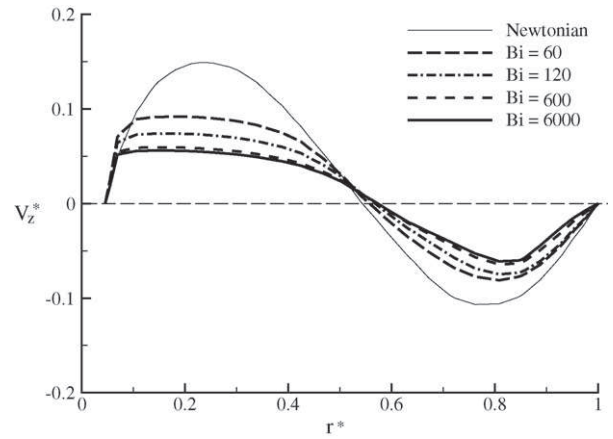


Fig. 2. Radial profiles of the axial velocity for Bingham fluids (double helical ribbon,  $z^* = 1, x^* = 0$ ).

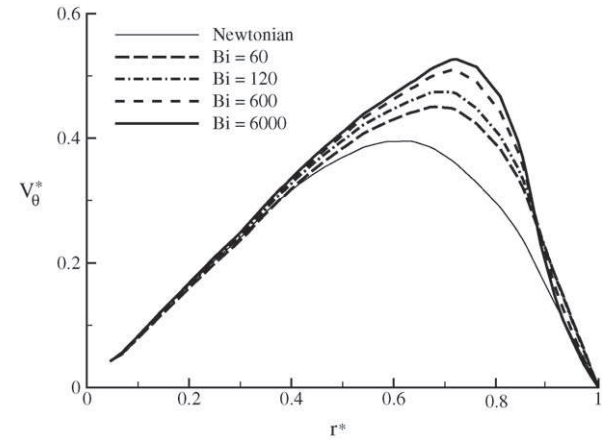


Fig. 3. Radial profiles of the tangential velocity for Bingham fluids (double helical ribbon,  $z^* = 1, x^* = 0$ ).

gential velocity on a vertical line crossing the ribbon (defined by  $x^* = 0$  and  $y^* = y/(T/2) = 0.746$ ).

To further investigate the effects of viscoplasticity, it is then worth comparing shear rate fields. As mentioned previously,

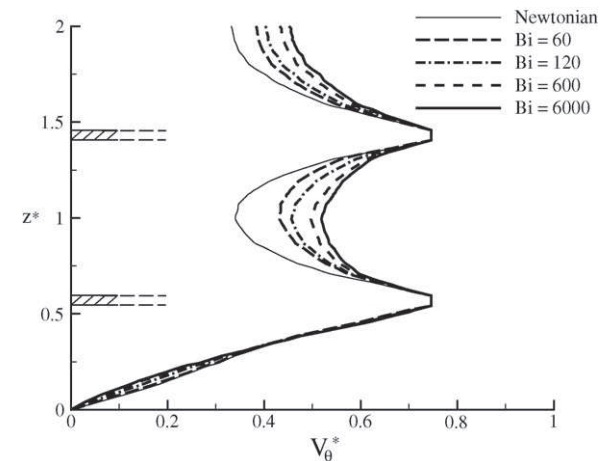


Fig. 4. Axial profiles of the tangential velocity for Bingham fluids (double helical ribbon,  $x^* = 0, y^* = 0.746$ ).

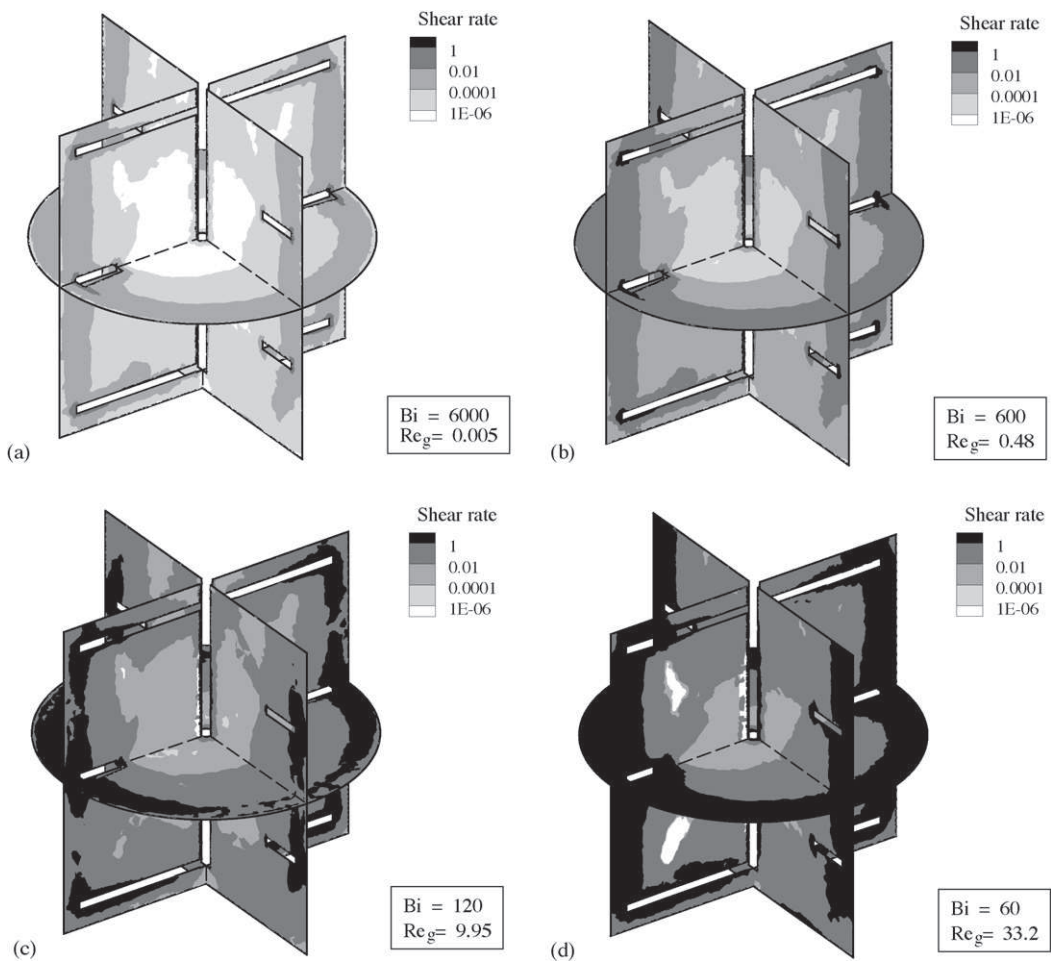


Fig. 5. Shear rate fields for Bingham fluids (double helical ribbon).

viscoplasticity has a major influence on hydrodynamics when parts of the flow domain experience stresses which are below the threshold. This leads to unsheared regions. Inversely, when shear stress is significantly higher than yield stress all over the domain, viscoplasticity is masked and the fluid behaves like a pseudoplastic fluid.

Thus shear rate  $\dot{\gamma}$  is a key parameter for both mixing efficiency and non-Newtonian behavior. Shear rate fields proceeding from 3D simulations with double helical ribbon are presented in Figs. 5 and 6. Fig. 5a–d present the viscoplastic Bingham case for Bingham numbers decreasing from 6000 to 60. Fig. 6a and b are for the Newtonian reference case. Similar results in a

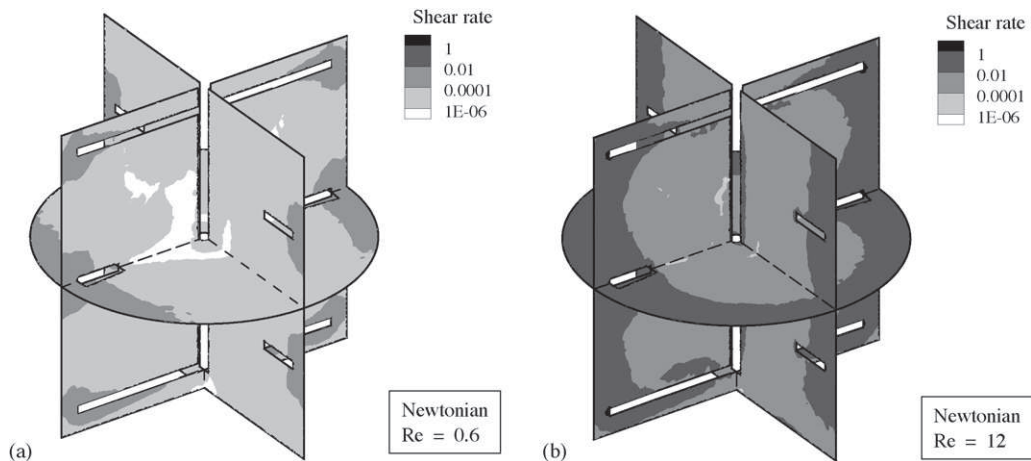


Fig. 6. Shear rate fields for Newtonian reference fluids (double helical ribbon).

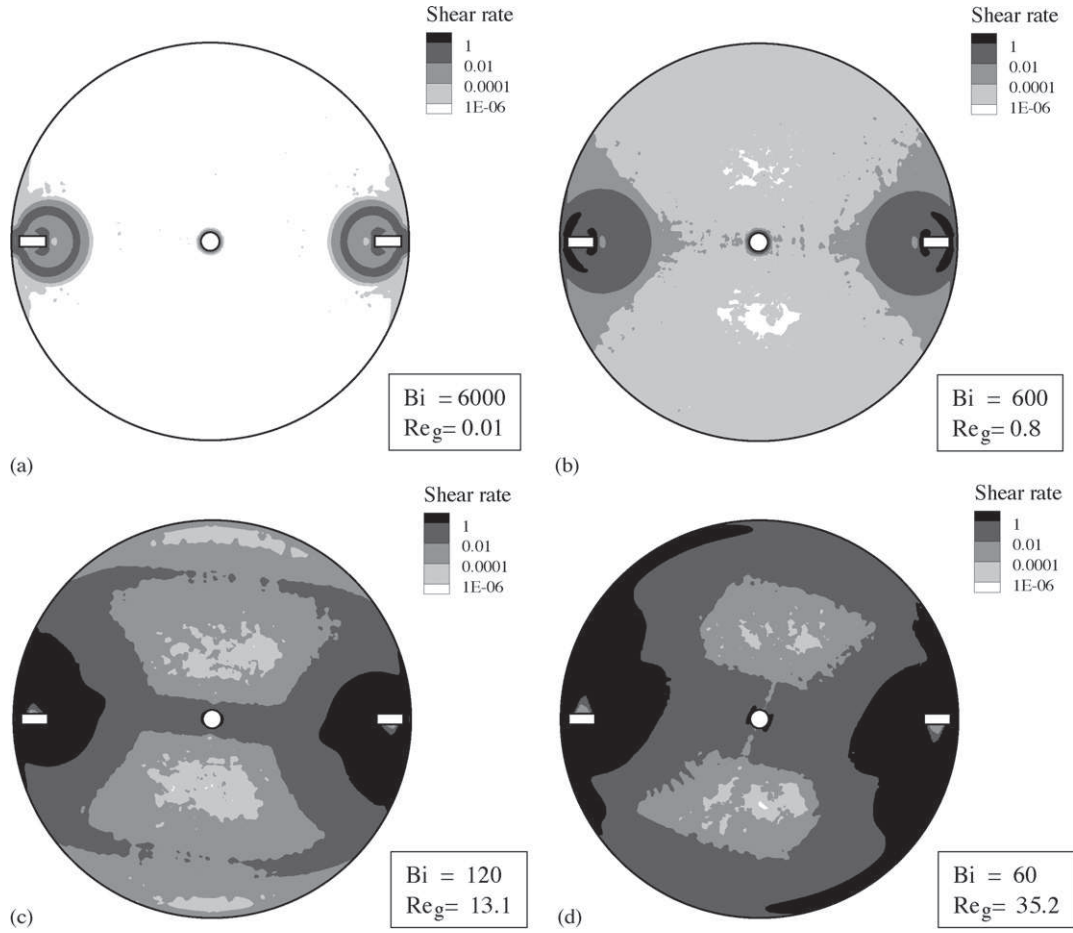


Fig. 7. Shear rate fields for Bingham fluids in a median horizontal plane (anchor agitator).

median horizontal plane for the anchor agitator are presented in Fig. 7a–d. The generalized Reynolds number  $Re_g$  mentioned in these figures is defined as the ratio  $K_p/N_p$ . The power consumption and, consequently, the power number  $N_p$  are calculated from the velocity field by the integration of viscous dissipation on the whole domain. The power constant  $K_p$  is determined with Newtonian cases and remains constant up to a Reynolds number of about 10. Values for each case are reported in Table 2 and agree with results from the literature.

In these representations of shear rate fields, the same color map divides the flow domain into five regions defined by the limiting values  $10^{-6} \text{ s}^{-1}$ ,  $10^{-4} \text{ s}^{-1}$ ,  $10^{-2} \text{ s}^{-1}$  and  $10^0 \text{ s}^{-1}$ . Figs. 5a and 7a reveal that a large part of the domain is almost shear-free for Bingham fluids (shear rate less than  $10^{-6} \text{ s}^{-1}$ ). Comparison with the Newtonian reference case (Fig. 6a and b for helical ribbon) confirms that hydrodynamics is governed independently by both the Bingham number and the generalized

Table 2  
Power constants (2D anchor: using  $H = T$ )

	$K_p$
2D anchor	246
3D anchor	334
Helical ribbon	325

Reynolds number (see differences between Figs. 5b and 6a, or between Figs. 5c and 6b, which are obtained for similar Reynolds values). This shows the influence of viscoplasticity on this flow which is then restricted to regions around the impeller for high Bingham numbers. The equivalent structure was found for the anchor agitator as described by Elson [3] or Hirata and Aoshima [2] for mixing of yield stress fluid with agitators such as the Rushton turbine, pitched blade turbine or marine propeller. If the mixing power is insufficient, the flow is limited to a cavern around the impeller and the surrounding fluid is at rest. As measured with LDA by Hirata and Aoshima [2], the cavern is of approximately constant size in the laminar regime and begins to increase in size for generalized Reynolds numbers larger than 30 (as in the case of the Rushton turbine and non-baffled tank). Hirata and Aoshima used a generalized Reynolds number based on the Metzner and Otto concept. However, although it is not mentioned in their paper, the given data permit an estimate of the Bingham number. This gives values between 3.6 ( $Re_g = 1$ ) and 1.4 ( $Re_g = 30$ ). Considering the results presented in Figs. 5a–d and 7a–d, numerical simulation reveals that these sheared regions slowly increase in size as observed in Ref. [2] for the caverns, but simultaneously, higher shear rates progressively occur in the shear-free region of Figs. 5a or 7a. When reaching a higher Reynolds number ( $Re_g = 10$ , Fig. 5c), the shear-free region no longer exists in Bingham fluid and the structure of

the flow is similar to the Newtonian case (Fig. 6b). Subsequently, shear stresses are higher than the yield stress throughout the domain so that the effects of viscoplasticity are not discernible and the fluid behaves like a shear thinning fluid for these flow conditions. The differences from the Newtonian case result from power-law behavior. Nagata et al. [25], in their numerical approach applied to several agitators including anchor and helical ribbon, showed the existence of a critical Reynolds number  $Re'$  beyond which there are no shear-free regions throughout the tank.  $Re'$  is based on the plastic viscosity  $\eta_\infty$  and linked to fluid and geometry parameters. Expressed with the Bingham number, this relation is written as  $\sqrt{Re'/Bi} = 1$ . For the four cases of Fig. 5, this quantity is equal to 0.014, 0.14, 0.70, and 1.41, respectively (and 0.002, 0.02, 0.58 and 2.3 in Fig. 7a–d). Thus, the Nagata criterion is valid as a first approximation taking account of the fact that the evolution of the shear-free region is progressive.

### 3. Power consumption and Metzner–Otto concept

Now our purpose is to explore how the power number varies with the yield stress, *i.e.* with the Bingham number. To achieve this, the mixing system hydrodynamics results presented in Section 2 are used to calculate the power consumption and the Metzner–Otto parameter  $K_s$ . In fact, a complex flow configuration has been observed in the shear rate distribution. In order to understand and analyze these results, the Taylor–Couette flow is used to establish a qualitative basis of interpretation. Indeed several authors have used this analogy to analyze flows in mixing systems (Thakur et al. [26], Bousmina et al. [27], Ait-Kadi et al. [18]). So this simple flow is examined prior to examining the standard mixing systems.

#### 3.1. Analytical Taylor–Couette flow

The velocity field for the basic Taylor–Couette flow is well-known for the standard viscoplastic models, but to the best of our knowledge, these data have not been used to examine the  $M$ – $O$  parameter. Therefore we now focus on the incompressible, isothermal and 2D flow between two concentric cylinders of height  $H$ , with no-slip condition on the cylinders. The outer cylinder is fixed, while a torque  $C$  is applied to the inner cylinder which has a rotation frequency  $N$ . A geometrical parameter  $s$  is defined by the inner to outer diameter ratio  $R_1/R_2$ .

The following results are established for Bingham fluids. Similar results are obtained for Herschel–Bulkley fluids (case  $n=1/2$  and  $n=1/3$ ) and Casson fluids. Constitutive equations and their subsequent results are presented in Appendix A (see Table A.1 for Bingham number definition). Velocity profiles for such fluids have already been presented by Bird, Dai and Yarusso [28] for a Bingham Fluid, or Jarny and Coussot [29] for Herschel–Bulkley fluids. Whatever the constitutive equation for the fluid is, the hydrodynamics for viscoplastic fluids depends on the torque  $C$  with two critical values:  $C_1 = 2\pi H\tau_0 R_1^2$  and  $C_2 = 2\pi H\tau_0 R_2^2$ . For lower torque ( $C \leq C_1 < C_2$ ), the shear stress imposed on the fluid is below the threshold  $\tau_0$  and, with no-slip boundary conditions, this leads to zero velocity over the

entire domain. For intermediate and higher torques, shear stress depends on the radial co-ordinate  $r^* = r/R_2$  and is a decreasing function of  $r^*$ .

Two cases are considered related to a critical radius  $X_0$ :

$$X_0 = \frac{1}{R_2} \sqrt{\frac{1}{2\pi H} \frac{C}{\tau_0}} \quad (7)$$

For intermediate torque ( $C_1 \leq C \leq C_2$ ), the shear stress is higher than the threshold  $\tau_0$  until  $r^*$  is lower than  $X_0$ . Conversely, the shear stress is lower than  $\tau_0$  for greater values of  $r^*$ . This flow will be called 'mixed flow' as the fluid is sheared in the region defined by  $r^* \leq X_0$  and motionless for  $r^* \geq X_0$ . Note that the previous condition for  $C$  is equivalent to the  $X_0$ -condition:  $s \leq X_0 \leq 1$ .

For higher torque ( $C \geq C_2 > C_1$ , equivalent to:  $X_0 \geq 1$ ), the whole domain is sheared. This kind of flow will be called 'fully sheared flow'. In this configuration, the shear rate is non-zero throughout the domain and the apparent behavior of the fluid is not fundamentally different from that of a corresponding shear thinning fluid.

It is noteworthy that  $X_0$  and the Bingham number are connected by a one to one relation (see Appendix A, Table A.2). The transition between mixed and fully sheared flows then occurs for  $X_0 = 1$  or, equivalently, for  $Bi = Bi^*$  with:

$$Bi^* = \frac{4\pi s^2}{1 - s^2 + 2s^2 \ln s} \quad (8)$$

The shear-free regions observed in mixing systems are similar to those of Taylor–Couette flow and we will now focus on power consumption in connection with hydrodynamics. Expression of the power consumption  $P$  for power-law fluids with power-law index  $n$  is given in [30] and this leads to  $K_s$  value for this geometry [7]:

$$K_s = 4\pi n^{n/(1-n)} \left( \frac{(1 - s^{2/n})^n}{1 - s^2} \right)^{1/(1-n)} \quad (9)$$

In addition, a weak dependence on  $n$  is observed as long as the ratio  $s$  is sufficiently high, thereby justifying a  $n$ -independency in the first approximation.

Now considering a Bingham fluid, the fact of expressing the generalized Reynolds number allows us to compute an effective viscosity  $\eta_{\text{eff}}$  for the flow. Using the constitutive Eq. (5) and relation (3) successively, we define an effective shear rate  $\dot{\gamma}_{\text{eff}}$  associated with the effective viscosity  $\eta_{\text{eff}}$  and finally the  $K_s$  expression for this geometry:

- For mixed flow ( $X_0 \leq 1$ ):

$$K_s = \frac{4\pi}{1 - X_0^2 + 2 \ln(X_0/s)} \quad (10)$$

- For fully sheared flow ( $X_0 \geq 1$ )

$$K_s = \frac{-2\pi}{\ln s} \quad (11)$$

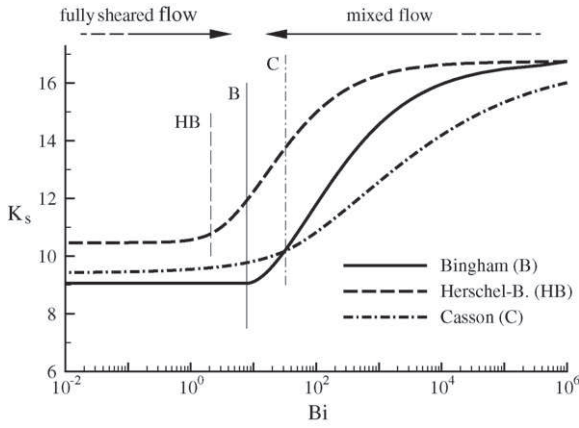


Fig. 8. Metzner–Otto parameter  $K_s$  for viscoplastic fluids in Taylor–Couette flow. Vertical lines: transition Bingham number  $Bi^*$  for the three models studied (case  $s=0.5$  for Bingham, Casson and Hershel Bulkley with  $n=0.5$ ).

So, for a Bingham fluid, the  $K_s$  value is constant for fully sheared flows (*i.e.* when  $C \geq C_2$  or  $Bi \leq Bi^*$ ) but depends on  $X_0$  (or  $C$ ) for mixed flows. Using the correspondence between  $X_0$  and the Bingham number  $Bi$ , Fig. 8 presents  $K_s$  versus  $Bi$  in the case of  $s=0.5$ . The transition between mixed flow and fully sheared flow is observed for  $Bi = Bi^*$ . To show the influence of the constitutive law,  $K_s$  versus  $Bi$  is also presented for the Herschel–Bulkley ( $n=0.5$ ) and Casson models in Fig. 8. Both the minimum  $K_s$  value and the transition Bingham number  $Bi^*$  depend on the model. It should be noted that, unlike the Bingham model, the Metzner–Otto parameter  $K_s$  is not constant when the flow is fully sheared for either the Hershel–Bulkley or Casson models but variations of  $K_s$  are weak and approximation by a constant value may be satisfactory in this case.

A preliminary conclusion is that the Metzner–Otto concept is valid for Bingham fluids insofar as the flow corresponds to a fully sheared regime, that is, when the fluid is used in its shear thinning domain. However,  $K_s$  variations increase when  $s$  decreases, and a constant  $K_s$  value can be quite acceptable for higher values of  $s$  (for instance: 25% variations for  $s=0.8$ ).

The great interest of the Metzner–Otto correlation is the prediction of power consumption and it is easy to use when  $K_s$  is constant. This is justified for power-law fluids but must be used with care for viscoplastic fluids when the flow is not fully sheared. For instance,  $K_s$  varies in a ratio of 1:2 when  $s=0.5$  and considering it as constant leads to significant errors on effective viscosity  $\eta_{eff}$  and on power consumption.

### 3.2. Numerical results for mixing system and discussion

Focusing now on the numerical results for the mixing systems under consideration, the Metzner–Otto parameter  $K_s$  was determined as described in Section 3.1 for the Couette flow. Fig. 9 presents  $K_s$  versus  $Bi$  in the laminar region for both double helical ribbon impeller and 2D and 3D anchors. Concerning numerical simulations conducted for the 2D anchor agitator, it is noteworthy that ( $K_s, Bi$ ) values are obtained with different rotation frequencies and different yield stresses, which confirms that  $K_s$  depends mainly on  $Bi$ . The large range of Bingham numbers

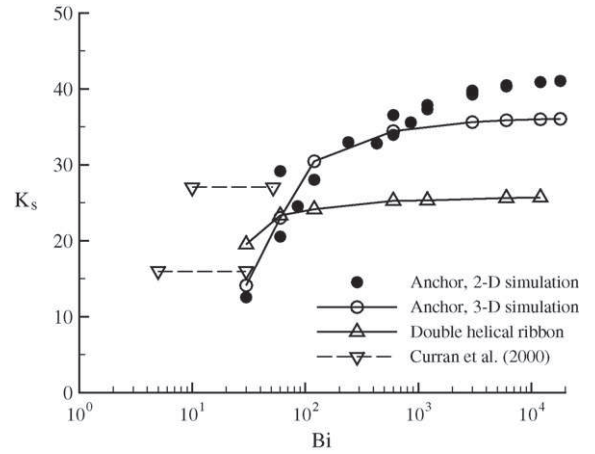


Fig. 9. Metzner–Otto parameter  $K_s$  for Bingham fluids in mixing systems.

explored, up to  $1.2 \times 10^4$ , reveals significant variations of  $K_s$  for the 2D anchor, corresponding to a ratio of 1:3.27 for the extreme values of  $Bi$ . Taking into account the 3D effects reduces these variations to a ratio of 1:2.55. The double helical ribbon gives weaker variations with a ratio of 1:1.32 although an asymptotic value for low Bingham numbers is not reached. The  $K_s$  versus  $Bi$  curve is therefore similar to that observed for the Taylor–Couette flow: a smoothly varying region for high Bingham numbers corresponding to a large shear-free region. Decreasing  $Bi$  leads to a transition region with noticeable  $K_s$  variations for Bingham numbers in the range 30–1000 (anchor) or 30–100 (double helical ribbon) where the shear rate progressively increases in the vessel while shear-free regions vanish.

Numerical results obtained by Bertrand et al. [13] for a 3D anchor agitator differ from ours as they indicate low variations of  $K_s$  in a ratio of 1:1.13 when the Bingham number varies from 8 to 7500. This latter conclusion does not agree with our observations for comparable configurations. However, the experimental results in literature do not justify the use of constant  $K_s$  on a large range of Bingham numbers. Indeed, the constant value of  $K_s$  used by Hirata and Aoshima [2] in their analysis is satisfactory because the Bingham number range explored is restricted (from 1.4 to 3.6). But experimental results obtained by Curran et al. [12] are particularly interesting as these authors studied the same double helical ribbon as we did, and observed non-negligible variations of  $K_s$ . Fitting their power number results, they obtain a mean value of  $K_s$  equal to 16 and 27 for each of the two fluids that they tested. Bingham numbers can be calculated for these experiments and lie in the range 5–30 for the first fluid ( $K_s = 16$ ), and 10–52 for the second fluid ( $K_s = 27$ ). These experimental values are reported in Fig. 5. It is worth noticing that they are close to the minimum and maximum values that we obtain numerically for the same geometry (19 and 26) although their experimental values are shifted towards lower Bingham numbers.

Thus the differences in the values of  $K_s$  with respect to the Bingham number  $Bi$  impose the use of a non-constant value in the Metzner–Otto correlation for a large  $Bi$  range. A generalized Reynolds number  $Re_g$ , which is linked to the fluid rheology, can be determined using the  $K_s$  parameter. Variations in the value

of  $K_s$  induce differences in the evaluation of  $Re_g$  and thus in the determination of the flow regime. The results of the present paper concord in a qualitative sense with the theoretical results obtained for the Taylor–Couette flow and are consistent with experimental observations. They can be retained as a working basis for the purpose of chemical engineering design.

#### 4. Conclusion

This numerical work has been developed in order to provide a physical analysis of mixing in viscoplastic fluids from the knowledge of local hydrodynamics and shear rate distributions. Large shear-free zones can appear in which the yield stress induces plug flows. This drastically changes the law of power consumption with respect to the Reynolds number. For this reason, we have examined the validity of the Metzner–Otto concept in a large range of Bingham and Reynolds numbers.

As a qualitative support to the analysis of mixing systems, the analytical results for the Taylor–Couette flow are used to express the power number as well as the  $K_s$  parameter for this specific flow. They show that  $K_s$  strongly depends on the Bingham number and on  $X_0$  critical radius delimiting the shear and shear-free regions. Such regions are observed in the studied mixing systems through the examination of the shear rate fields.

After examination of two standard agitators for high viscosity fluids (double helical ribbon and anchor), it can be concluded that a constant value for the Metzner–Otto parameter  $K_s$  is not

a reasonable option when the Bingham number varies significantly. These results are coherent with the experimental results presented in literature. On the basis of this analysis it is clear that a variation of  $K_s$  must be taken into account and that it would be very useful to improve the knowledge of hydrodynamics, particularly the sheared/unsheared region distribution, in order to provide a predictive tool for designers.

#### Acknowledgement

This project was partly financed by a grant from the Joint Program Research FERMaT (‘Fédération pour l’Etude des Réacteurs et la Maîtrise des Transferts’).

#### Appendix A

Additional results for Bingham fluids and results for Herschel-Bulkley and Casson fluids are given in Tables A.1–A.3.

##### A.1. Metzner–Otto parameter $K_s$ for general Herschel-Bulkley fluid

For the general case of Herschel-Bulkley model (*i.e.* whatever  $n$  is), a simple analytic expression does not exist for  $K_s$  for the Taylor–Couette flow. But it is easy to demonstrate existence and uniqueness for  $K_s$ . Thus, determining velocity field in

Table A.1  
Herschel-Bulkley and Casson fluids: constitutive law and Bingham number definition

	Herschel-Bulkley fluid	Casson fluid
Model: Eq. (4) and, for $\tau \geq \tau_0$	$\underline{\tau} = \left( K \dot{\gamma}^{n-1} + \frac{\tau_0}{\dot{\gamma}} \right) \underline{D}$	$\underline{\tau} = \left( K_c + \sqrt{\frac{\tau_0}{\dot{\gamma}}} \right)^2 \underline{D}$
$Bi$	$\frac{\tau_0}{K N^n}$	$\frac{\tau_0}{K_c^2 N}$

Table A.2  
Relation between Bingham number and  $X_0$  parameter for Taylor–Couette flow defined in Section 2.2

	Mixed flow ( $s \leq X_0 \leq 1$ )	Fully sheared flow ( $X_0 \geq 1$ )
Bingham	$Bi = \frac{4\pi}{(X_0^2/s^2) - 1 - 2 \ln(X_0/s)}$	$Bi = \frac{4\pi}{(X_0^2/s^2) - X_0^2 + 2 \ln s}$
Herschel-Bulkley ( $n = 1/2$ )	$Bi = \frac{(2\pi)^{1/2}}{((1/4)(X_0^4/s^4) - (X_0^2/s^2) + (3/4) + \ln(X_0/s))^{1/2}}$	$Bi = \frac{(2\pi)^{1/2}}{((1/4)(X_0^4/s^4)(1 - s^4) - (X_0^2/s^2)(1 - s^2) - \ln s)^{1/2}}$
Casson	$Bi = \frac{4\pi}{(X_0^2/s^2) - 4(X_0/s) + 3 + 2 \ln(X_0/s)}$	$Bi = \frac{4\pi}{(X_0^2/s^2)(1 - s^2) - 4(X_0/s)(1 - s) - 2 \ln s}$

Table A.3  
Metzner–Otto parameter  $K_s$  for Herschel-Bulkley and Casson fluids

	$K_s$	$K_{s,min}$
Herschel-Bulkley ( $n = 1/2$ )	$K_s = \frac{4\pi^2 s^4}{Bi^2 X_0^4 (1 - s^2)^2} \left( 1 + \sqrt{1 + \frac{1}{\pi} Bi^2 \frac{X_0^2}{s^2} (1 - s^2)} \right)^2$	$2\pi \frac{1 + s^2}{1 - s^2}$
Casson	$K_s = 4\pi \frac{Bi}{(X_0^2/s^2)(\sqrt{Bi(1 - s^2)} - \sqrt{4\pi(s/X_0)})^2}$	$\pi \frac{1 + s}{1 - s}$

Newtonian case leads to:

$$N = \frac{C}{8\pi^2 HR_2^2 \eta} \frac{1 - s^2}{s^2} \quad (\text{A.3})$$

For viscoplastic fluids,  $\eta_{\text{eff}}$  is defined as the Newtonian viscosity leading to the same power consumption. Eq. (A.3) then applied for  $\eta = \eta_{\text{eff}}$ . Together with Eq. (7) to express the torque  $C$  and using the constitutive law (Table A.1), one obtains:

$$\frac{1}{4\pi} \frac{1 - s^2}{s^2} Bi X_0^2 K_s - K_s^n - Bi = 0 \quad (\text{A.4})$$

For fixed values of  $s$ ,  $X_0$  and  $Bi$ , Eq. (A.4) has a single positive  $K_s$ -solution. As a complementary result (A.5) gives:

$$K_{s,\text{max}} = \frac{4\pi}{1 - s^2}. \quad (\text{A.5})$$

## References

- [1] F. Ein-Mozaffari, C.P.J. Bennington, G.A. Dumont, Suspension yield stress and the dynamic response of agitated pulp chests, *Chem. Eng. Sci.* 60 (2005) 2399–2408.
- [2] Y. Hirata, Y. Aoshima, Formation and growth of cavern in yield stress fluids agitated under baffled and non-baffled conditions, *Chem. Eng. Res. Des.* 74 (4) (1996) 438–444.
- [3] T.P. Elson, The growth of caverns formed around rotating impellers during the mixing of a yield stress fluid, *Chem. Eng. Commun.* 96 (1990) 303–319.
- [4] A.B. Metzner, R.E. Otto, Agitation of non-Newtonian fluids, *AIChE J.* 3 (1) (1957) 3–10.
- [5] P.A. Tanguy, F. Thibault, E. Brito De La Fuente, A new investigation of the Metzner–Otto concept for anchor mixing impellers, *Can. J. Chem. Eng.* 74 (1996) 525–532.
- [6] D. Doraiswamy, R.K. Grenville, A.W. Etchells, Two-score years of the Metzner–Otto correlation, *Ind. Eng. Chem. Res.* 33 (1994) 2253–2258.
- [7] E. Brito De La Fuente, L. Choplin, P.A. Tanguy, Mixing with helical ribbon impellers: effect of highly shear thinning behaviour and impeller geometry, *Chem. Eng. Res. Des.* 75 (1) (1997) 45–52.
- [8] P.J. Carreau, R.P. Chhabra, J. Cheng, Effect of rheological properties on power consumption with helical ribbon agitators, *AIChE J.* 39 (9) (1993) 1421–1430.
- [9] F. Rieger, V. Novak, Power consumption of agitators in highly viscous non-Newtonian liquids, *Trans. Inst. Chem. Eng.* 51 (1973) 105–111.
- [10] J. Sestak, R. Zitny, M. Houska, Anchor-agitated systems: power input correlation for pseudoplastic and thixotropic fluids in equilibrium, *AIChE J.* 32 (1) (1986) 155–158.
- [11] S. Nagata, M. Nishikawa, H. Tada, H. Hirabayashi, S. Gotoh, Power consumption of mixing impellers in Bingham plastic liquids, *J. Chem. Eng. Jpn.* 3 (2) (1970) 237–243.
- [12] S.J. Curran, R.E. Hayes, A. Afacan, M. Williams, P. Tanguy, Experimental mixing of a yield stress fluid in a laminar stirred tank, *Ind. Eng. Chem. Res.* 39 (2000) 195–202.
- [13] F. Bertrand, P.A. Tanguy, E. Brito De La Fuente, A new perspective for the mixing of yield stress fluids with anchor impellers, *J. Chem. Eng. Jpn.* 29 (1) (1996) 51–58.
- [14] P.A. Tanguy, F. Bertrand, R. Labrie, E. Brito De La Fuente, Numerical modelling of the mixing of viscoplastic slurries in a twin-blade planetary mixer, *Trans. IChemE* 74 (A) (1996) 499–504.
- [15] C. Torrez, C. Andre, Simulation of a Rushton turbine mixing yield stress fluids: application of the Metzner–Otto concept, *Chem. Eng. Technol.* 22 (8) (1999) 701–706.
- [16] M. Marouche, D. Anne-Archard, M. Sengelin, H.C. Boisson, Hydrodynamics of emulsion polymerization at high concentration: effect of non-Newtonian characteristics, in: *Proceedings of the 14th International Congress of Chemical and Process Engineering CHISA, Praha, Czech Republic, August 27–31, 2000.*
- [17] M. Marouche, D. Anne-Archard, H.C. Boisson, A numerical model of yield stress fluid dynamics in a mixing vessel, *Appl. Rheol.* 12 (4) (2002) 182–191.
- [18] A. Ait-Kadi, P. Marchal, L. Choplin, A.S. Chrissemant, M. Bousmina, Quantitative analysis of mixer-type rheometers using the Couette analogy, *Can. J. Chem. Eng.* 80 (6) (2002) 1166–1174.
- [19] G.C. Vradis, M.V. Otugen, The axisymmetric sudden expansion flow of a non-Newtonian viscoplastic fluid, *J. Fluid Eng.* 119 (1997) 193–200.
- [20] E.J. O’Donovan, R.I. Tanner, Numerical analysis of the Bingham squeeze film problem, *J. Non-Newtonian Fluid Mech.* 15 (1984) 75–83.
- [21] T.C. Papanastasiou, Flows of materials with yields, *J. Rheol.* 31 (5) (1987) 385–404.
- [22] T.V. Pham, V. Mitsoulis, Viscoplastic flows in ducts, *Can. J. Chem. Eng.* 76 (1998) 120.
- [23] M. Bercovier, M. Engelman, A finite element method for incompressible non-Newtonian flows, *J. Comput. Phys.* 36 (1980) 313–326.
- [24] M. Marouche, Hydrodynamique d’un système d’agitation en fluide viscoplastique et en régime laminaire inertiel, Thèse de Doctorat de l’INP Toulouse, France, 2002.
- [25] S. Nagata, M. Nishikawa, T. Katsube, K. Takaish, Mixing of highly viscous non-Newtonian liquids, *Int. Chem. Eng.* 12 (1) (1972) 175–182.
- [26] R.K. Thakur, C. Vial, G. Djelveh, M. Labbafi, Mixing of complex fluids with flat-bladed impeller: effect of impeller geometry and highly shear-thinning behaviour, *Chem. Eng. Process.* 43 (2004) 1211–1222.
- [27] M. Bousmina, A. Ait-Kadi, J.B. Faisant, Determination of shear rate and viscosity from batch mixer data, *J. Rheol.* 43 (2) (1999) 415.
- [28] R.B. Bird, G.C. Dai, B.J. Yarusso, The rheology and flow of viscoplastic materials, *Rev. Chem. Eng.* 1 (1) (1983) 1–70.
- [29] S. Jarny, P. Coussot, Caractérisation des écoulements de pâte dans une géométrie Couette, *Rhéologie* 2 (2002) 52–63.
- [30] J.R. Bourne, H. Butler, Power consumption of helical ribbon impellers in viscous liquids, *Trans. Inst. Chem. Eng.* 47 (1969) T263–T270.